Comparison of Stratus Cloud Microphysical Retrievals that Utilize Radar, Microwave Radiometer, and Pyranometer Measurements

X. Dong
Analytical Services and Materials, Inc.
Hampton, Virginia

P. Minnis
National Aeronautics and Space Administration
Langley Research Center
Hampton, Virginia

E. E. Clothiaux
Department of Meteorology
The Pennsylvania State University
University Park, Pennsylvania

G. G. Mace
Meteorology Department
University of Utah
Salt Lake City, Utah

J. C. Liljegren
Ames Laboratory
Ames, Iowa

Introduction

Three methods for inferring cloud layer-mean droplet effective radius (re) and cloud optical depth from radar, Microwave Radiometer (MWR), and pyranometer measurements are applied to data from 140 hours of isolated boundary-layer stratus clouds that occurred during the winter of 1997-1998 at the Atmospheric Radiation Measurement (ARM) Program's Southern Great Plains (SGP) site. Method 1 (M1) relies on radar reflectivity alone, whereas an alternative approach (Method 2 [M2]) uses radar reflectivity in combination with MWR retrievals of the liquid water path (LWP). The final method (Method 3 [M3]) is based on matching pyranometer measurements with the surface irradiance computed from a 2-stream radiative transfer model that incorporates the MWR LWPs. The goals of this study are to retrieve isolated boundary layer stratus cloud microphysics from radar, lidar, MWR and other measurements, to study the reliability of radar retrievals under different cloud conditions.

Data and Methods

The ground-based measurements at the ARM SGP site are cloud top height, cloud base height, cloud LWP, and downward solar flux at the surface. These measurements are obtained from a 35-GHz Millimeter Wave Cloud Radar (MMCR), a laser ceilometer, a multi-channel MWR, and an Eppley precision spectral pyranometer (PSP), respectively. About 140 hours of data from December 1997 to February 1998 have been used to study the statistical information about the stratus cloud microphysical retrievals from different approaches.

The first and second methods use the radar/lidar and radar/lidar/radiometer measurements to infer vertical profiles of cloud liquid water content (LWC) and re, then the vertical profiles have been averaged to the layer-mean to compare with the retrievals from the third method. M1 uses the radar reflectivity with the lidar detected cloud base height. The equations for this approach are

$$\mathrm{LWC}_1(z) = 0.302\,\rho_w\;N\,Z(z) \tag{1}$$

and

$$Z(z) = 2^6\;N < r^6 > = 2^6\;N\,re^6{}_1(z)\exp[3\,\sigma_x{}^2], \tag{2}$$

where σ_x (= 0.35) is the logarithmic width of the particle size distribution, N is the layer-mean cloud droplet number concentration obtained from the 2-stream radiative transfer model retrievals (Dong et al. 1997), and ρ_w is liquid water density. The cloud LWP can also be estimated by the radar reflectivity from Eq. (1). M2 (Frisch et al. 1995, 1998) uses a combination of radar reflectivity, laser ceilometer cloud base height, and MWR LWP measurements. The cloud base heights obtained from the laser ceilometer are used to filter out clutter and drizzle in the radar returns from below cloud base. The MWR-derived cloud LWPs are used as a constraint on the vertical sum of the derived cloud LWCs. The equations of M2 are

$$\mathrm{LWC}_2(z) = \frac{\mathrm{LWP}}{\mathrm{dH}}\,\frac{Z^{1/2}(z)}{\sum_{Zb}^{Zt} Z^{1/2}(z)} \tag{3}$$

and

$$re_2(z) = \left[\frac{\pi}{48}\exp\left(-6\sigma_x^2\right)\mathrm{dH}\right]^{1/3}\frac{\sum_{Zb}^{Zt} Z^{1/2}(z)}{\mathrm{LWP}} \tag{4}$$

where dH (=45 m) is the vertical extent of the radar sample volume and $\left[\sum_{Zb}^{Zt} Z^{1/2}(z)\right]$ represents the integrated radar reflectivity through the vertical extent of the cloud.

M3, which is independent of cloud droplet size distribution, is to retrieve the microphysical and radiative properties of stratus clouds by modifying a 2-stream radiative transfer model from the ground-based measurements (Dong et al. 1997). These ground-based measurements and retrievals have been parameterized as a function of the cloud LWP, the transmission ratio (the ratio of surface irradiance during cloudy conditions to the expected clear-sky surface irradiance), and the cosine of the solar zenith angle (Dong et al. 1998). This method is mainly dependent of the column measurements of cloud LWP and solar transmission, which are not too sensitive to the drizzles and ice particles if the water droplets are dominant. However, the radar reflectivity is proportional to the 6th power of cloud particle size, only a few large drizzles or ice particles can make huge radar reflectivity, which leads to overestimate cloud retrievals.

Results and Discussion

To illustrate the relationship between cloud retrievals with radar reflectivity, consider Figure 1. Figure 1 shows the retrieved cloud LWC and re as a function of radar reflectivity with the different cloud droplet concentrations (from Eqs. [1] and [2]), where the LWC and re increase significantly with increased radar reflectivity. Figure 2 shows the radar images for the cases with and without drizzles in this study. By comparing the retrieved re from M1 and M2 to those from M3, there are three kinds of results: smaller, comparable, and much larger with drizzles. Figures 3 and 4 show the retrieved results from three methods, where the re from M1 (Radar) and M2 (Radar_MWR) are smaller than those from M3 (2-stream). LWPs estimated from radar reflectivity (Radar) are also smaller than those from the MWR. Cloud optical depth is calculated by

$$\tau = \frac{3}{2}\frac{\mathrm{LWP}}{\mathrm{re}} \, , \qquad (5)$$

where only M1 uses the radar-estimated LWP. Both M2 and M3 use MWR measurements. The optical depths from M1 are smaller, while the optical depths from M2 are much larger than those from M3 due to the smaller re from M2. The layer-mean radar reflectivities are the average of radar data (Radar), and calculated from Eq. (2) with the inputs of retrievals from M3 (2-stream). One of the possible reasons for leading to smaller re from M1 and M2 is the assumed constant cloud droplet size distribution. The comparison results from these three methods are shown in Figures 5 and 6, and the larger re from M1 and M2 during the drizzle time period are shown in Figures 7, 8, and 9.

Comparison of the retrieval results reveals that M1 and M2 are generally in good agreement with M3 when the stratus are not drizzling (Figure 10). When drizzle occurs, the re and optical depths produced by M1 are larger than the values produced by M3, whereas M2 yielded re and optical depths that are respectively much larger and smaller than those from M3. These differences are partly due to the result of a dependence of the radar reflectivity on the 6th power of the cloud droplet re, while the liquid water content has only a dependence on the 3rd power of the re. Cloud droplet size distribution, which affects the radar retrieval, is another factor to the difference, especially for the cases on December 3, and December 25, 1997.

References

Dong, X., T. P. Ackerman, and E. E. Clothiaux, 1998: Parameterizations of microphysical and shortwave radiative properties of boundary layer stratus from ground-based measurements. *J. Geophys. Res.*, **103**, 31,695-31,694.

Dong, X., T. P. Ackerman, E. E. Clothiaux, P. Pilewskie, and Y. Han, 1997: Microphysical and radiative properties of boundary layer stratiform clouds deduced from ground-based measurements. *J. Geophs. Res.*, **102**, 23,829-23,843.

Frisch, A., C. W. Fairall, and J. B. Snider, 1995: Measurement of stratus cloud and drizzle parameters in ASTEX with a K-band Doppler radar and a microwave radiometer. *J. Atmos. Sci.*, **32**, 2788-2799.

Frisch, A., G. Feingold, C. W. Fairall, T. Utall, and J. B. Snider, 1998: On cloud radar and microwave radiometer measurements of stratus cloud liquid water profiles. *J. Geophs. Res.*, **103**, 23,195-23,197.

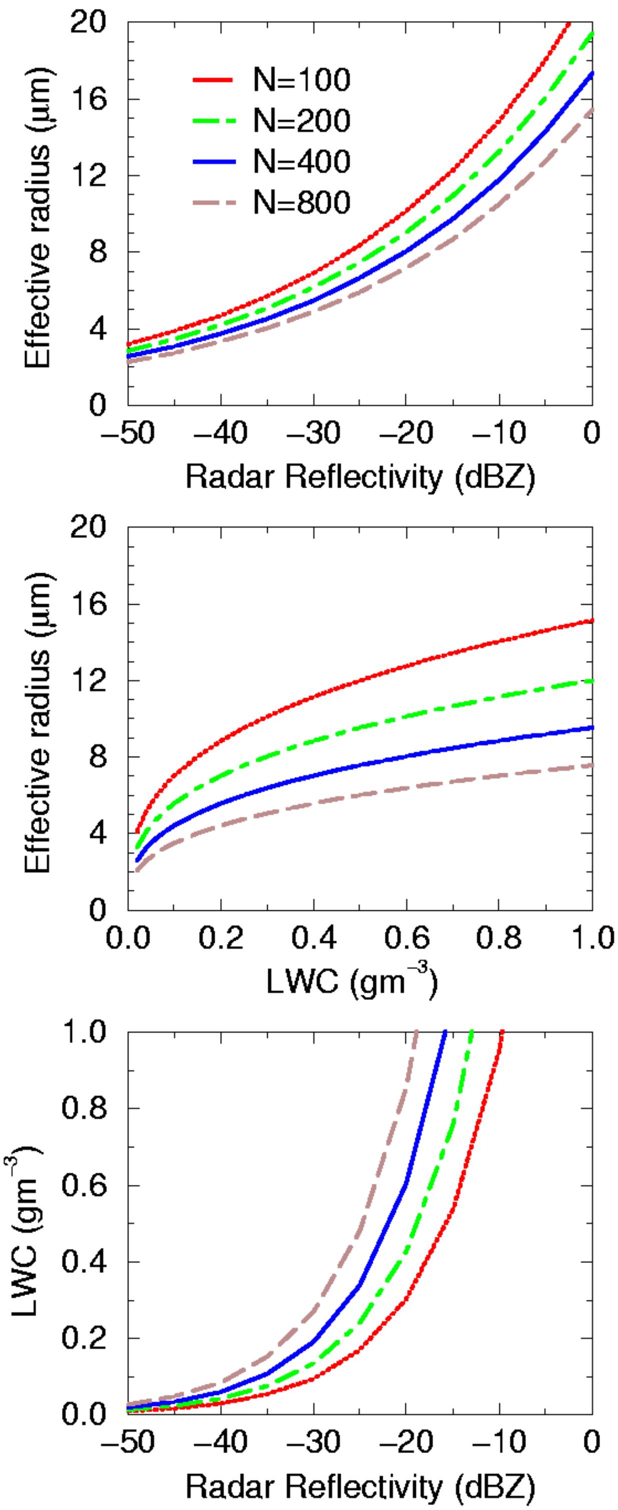

Figure 1. Simulation of radar retrievals from Eqs. (1) and (2).

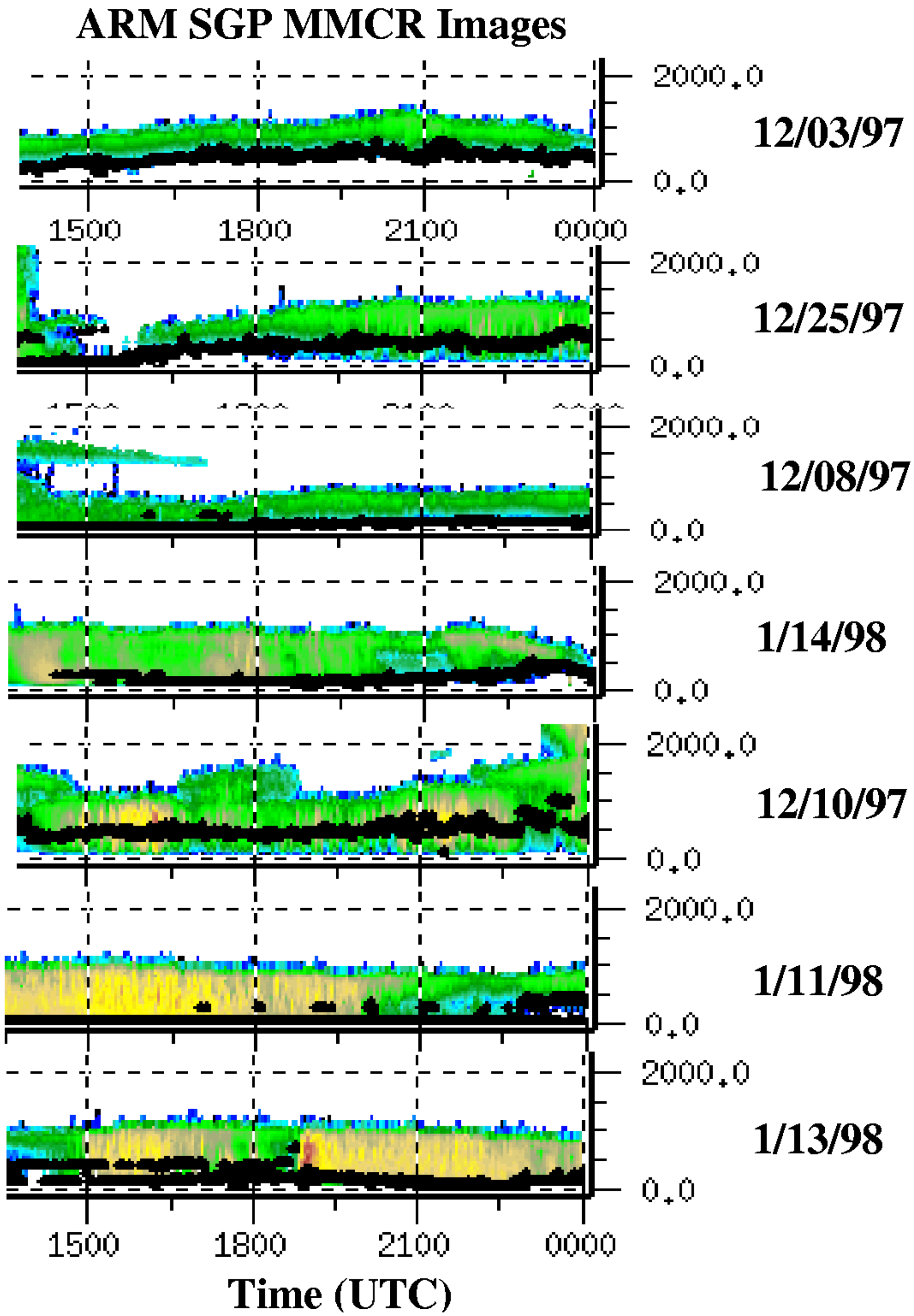

Figure 2. U.S. Department of Energy (DOE) ARM microwave cloud radar images.

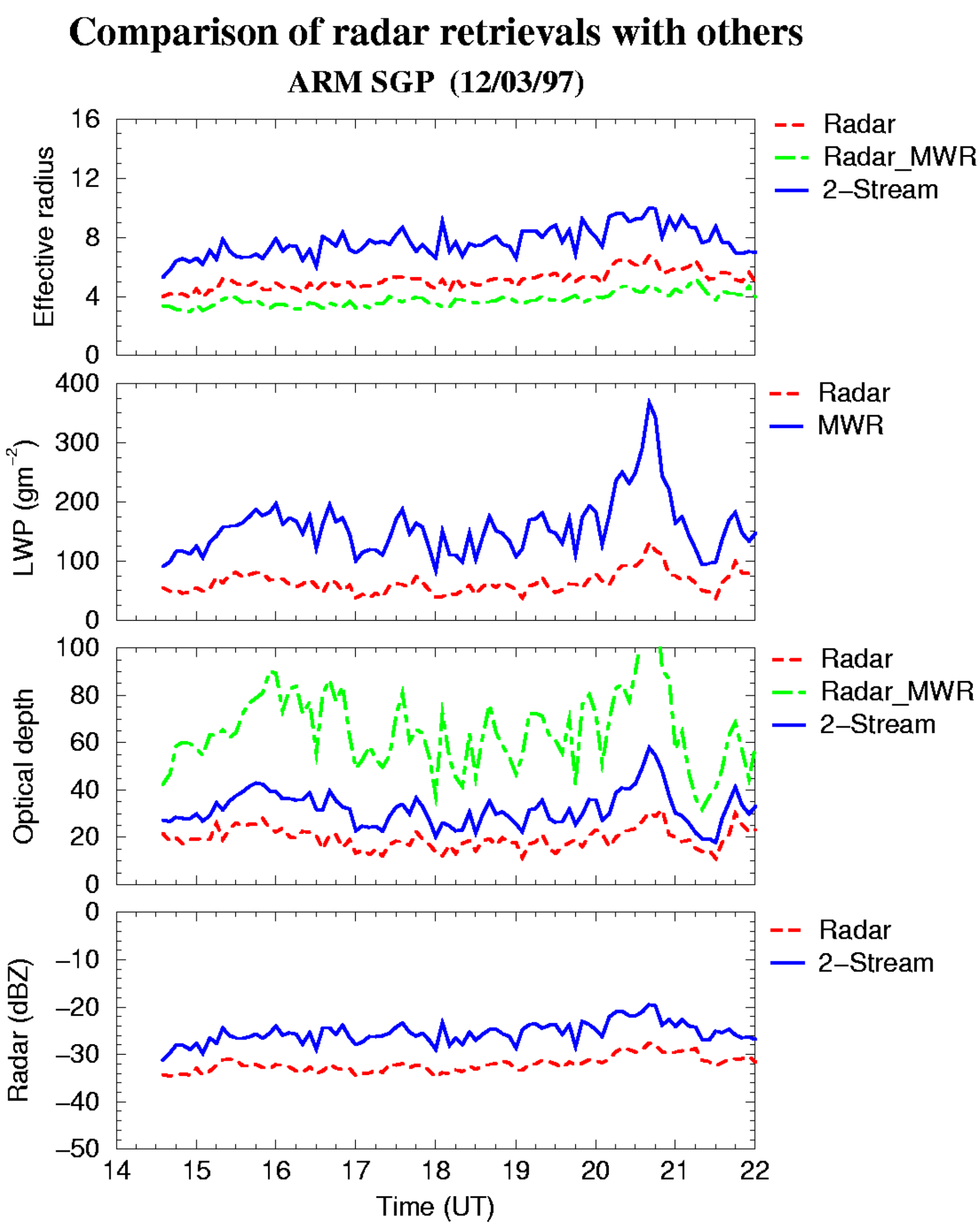

Figure 3. Comparison between M1 (Radar), M2 (Radar_MWR), and M3 (2-stream) on December 3, 1997.

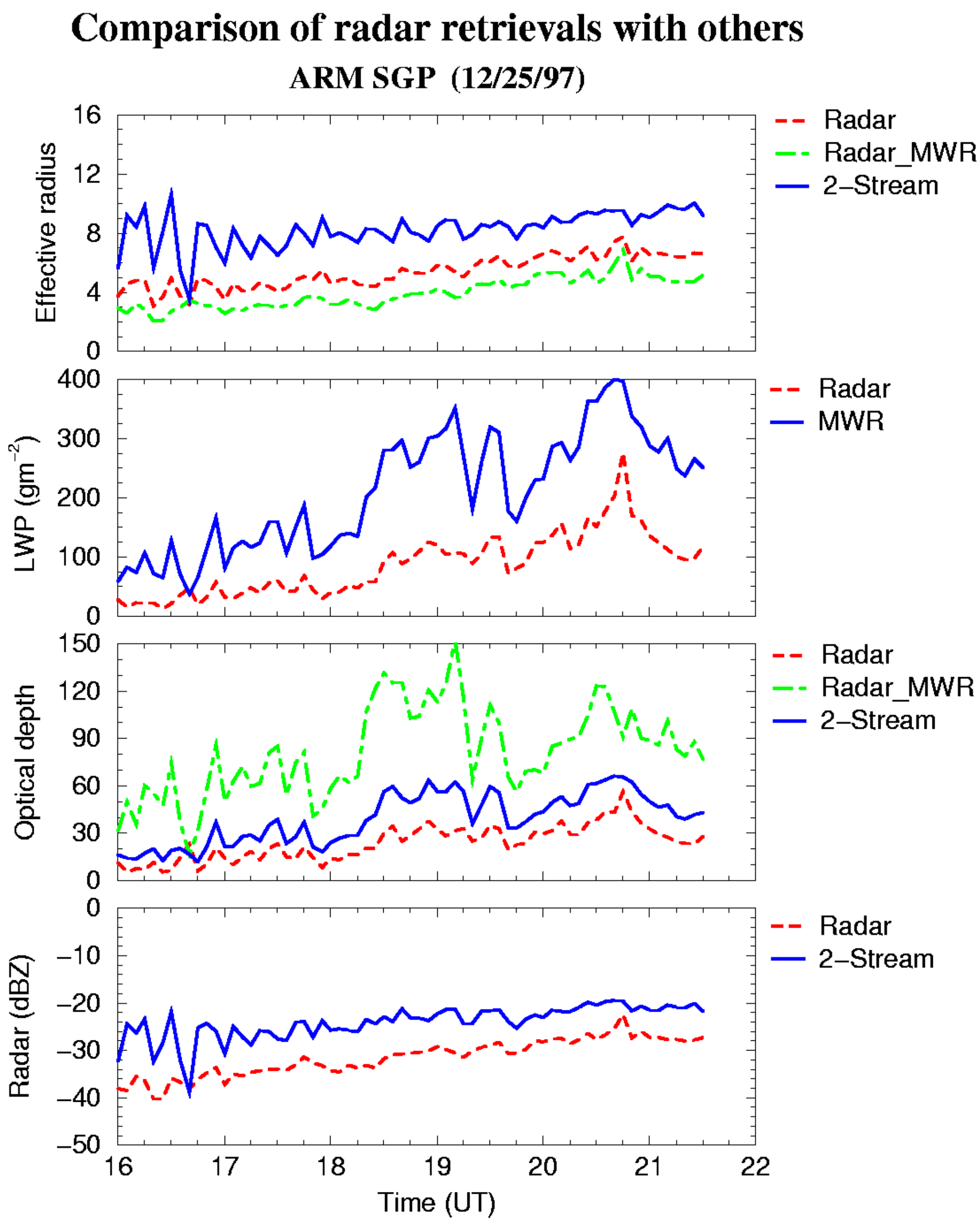

Figure 4. Same as Figure 3 but on December 25, 1997.

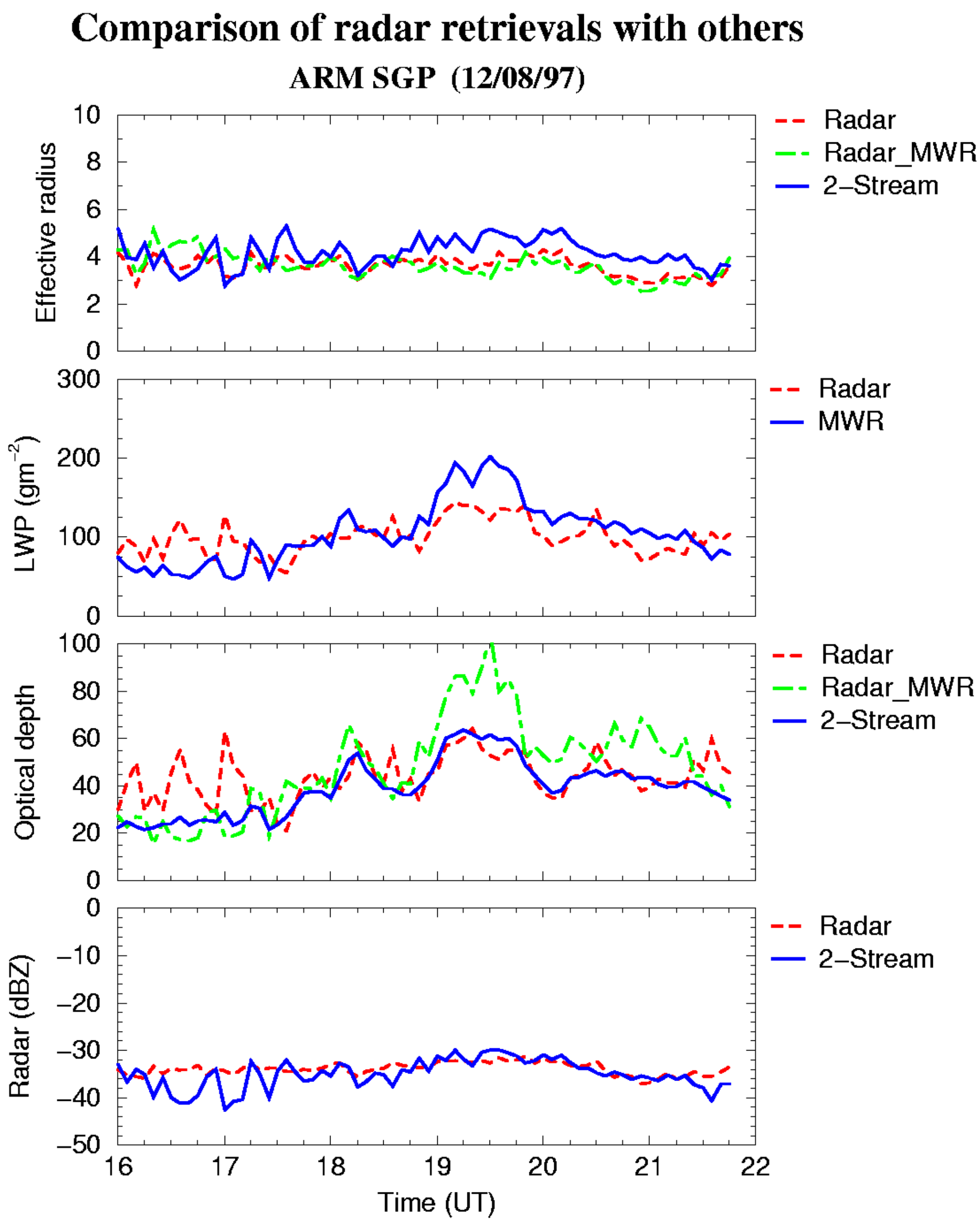

Figure 5. Same as Figure 3 but on December 8, 1997.

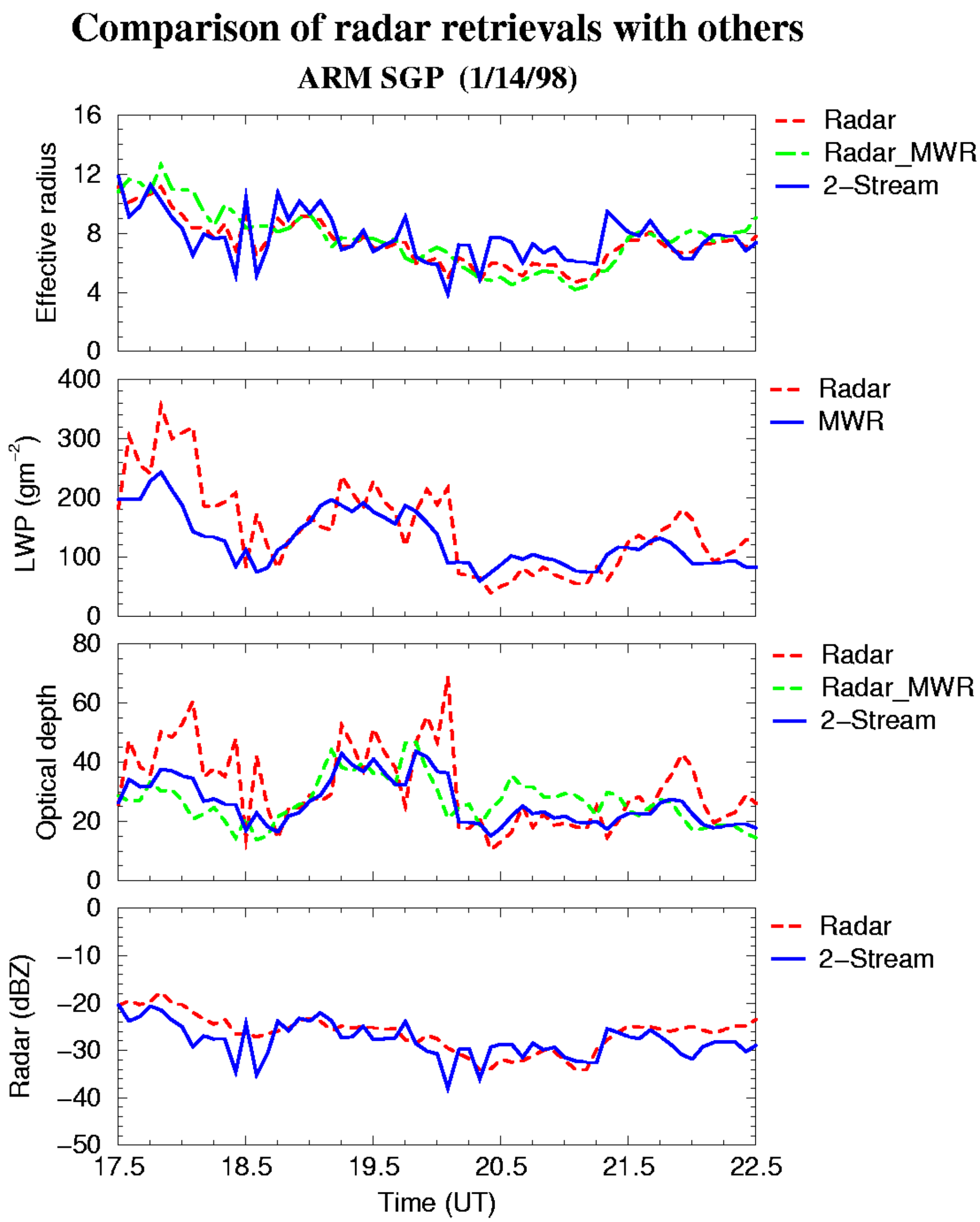

Figure 6. Same as Figure 3 but on January 14, 1998.

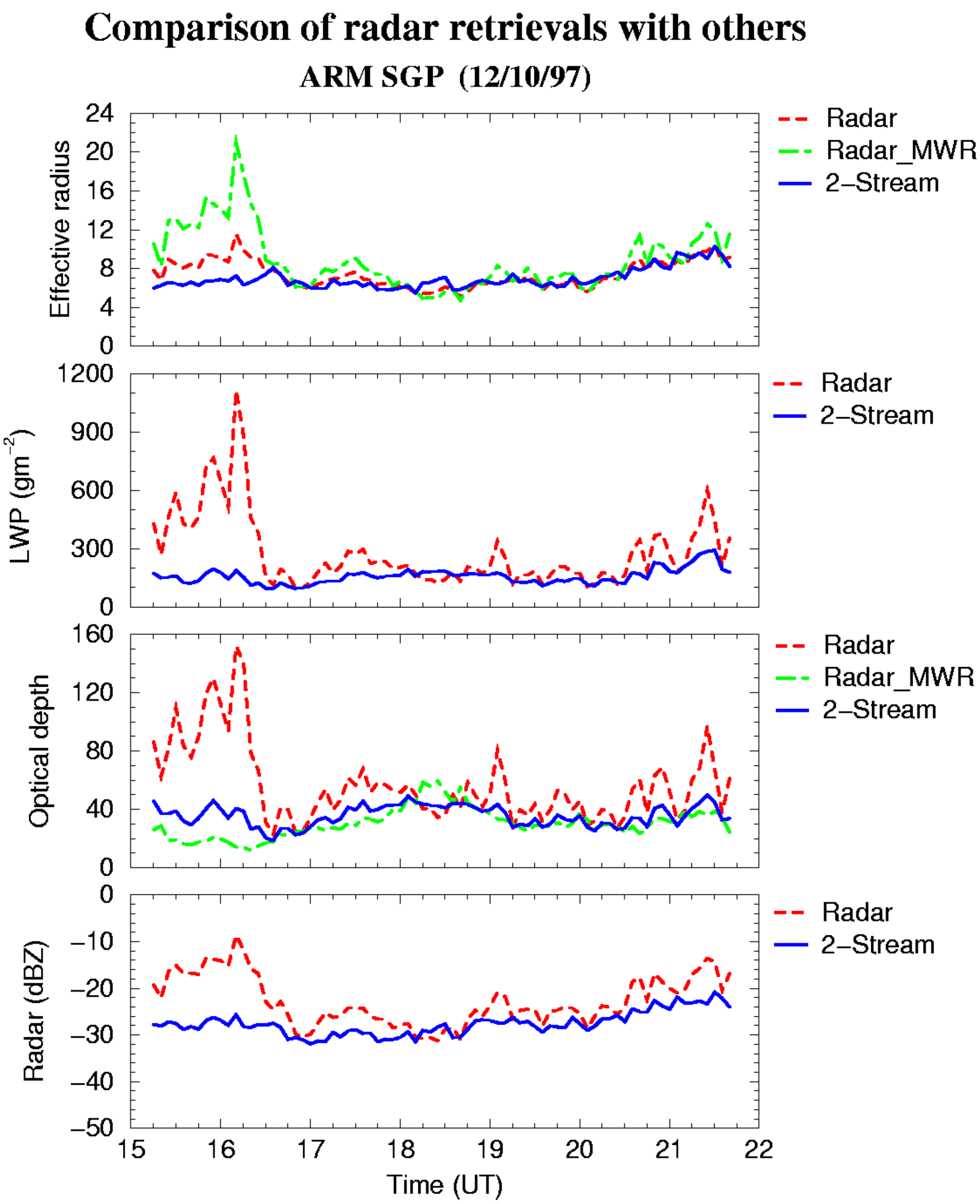

Figure 7. Same as Figure 3 but on December 10, 1997.

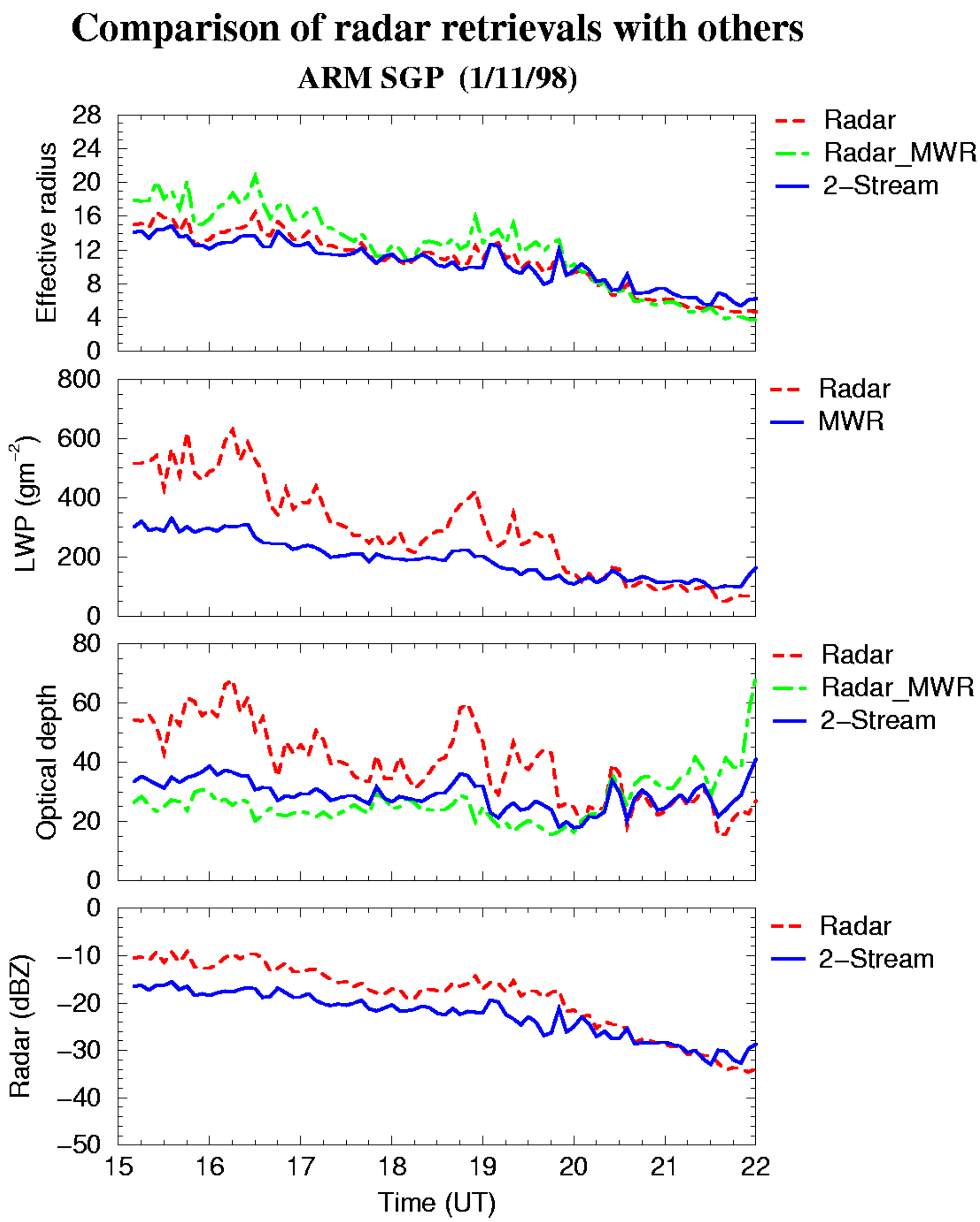

Figure 8. Same as Figure 3 but on January 11, 1998.

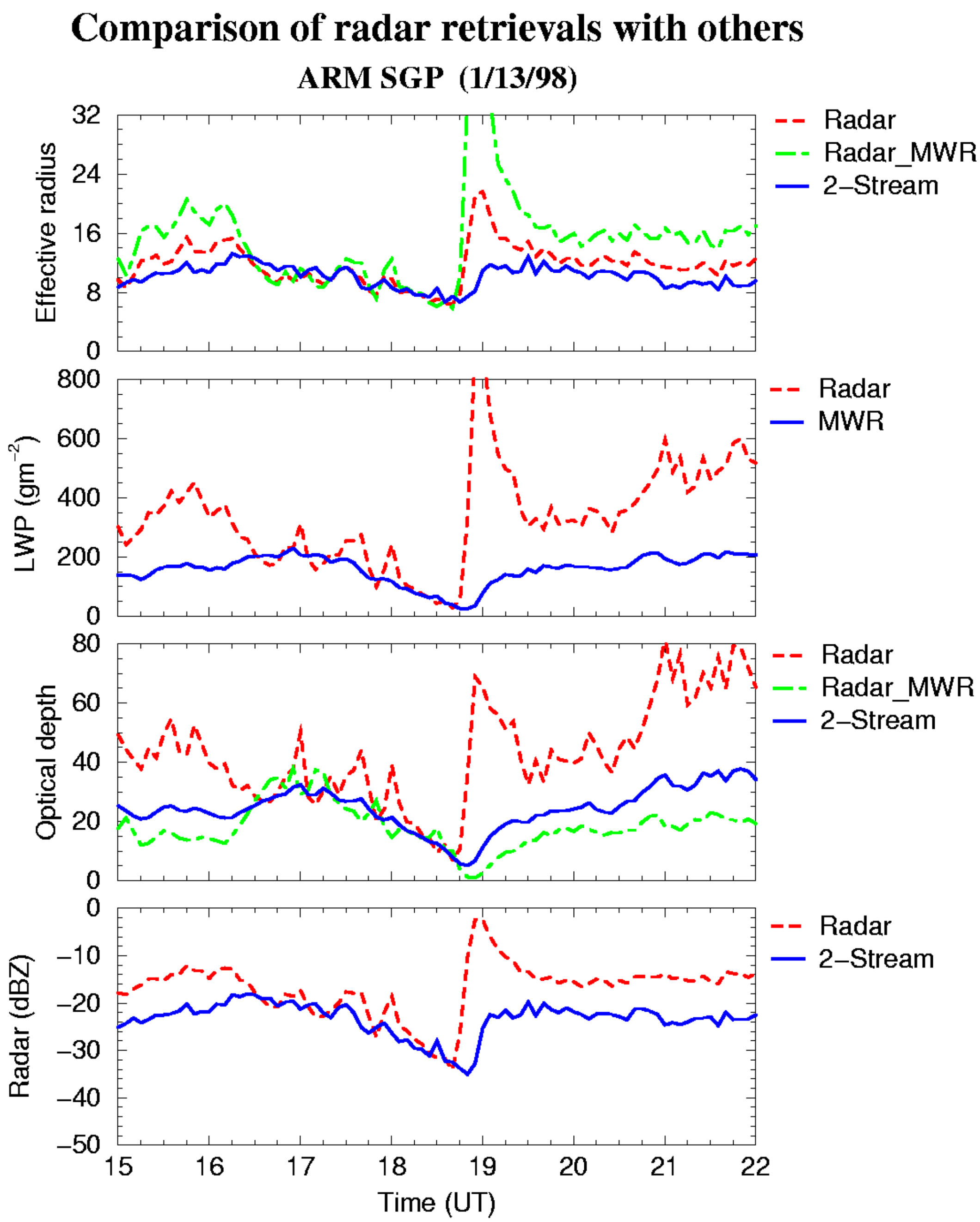

Figure 9. Same as Figure 3 but on January 13, 1998.

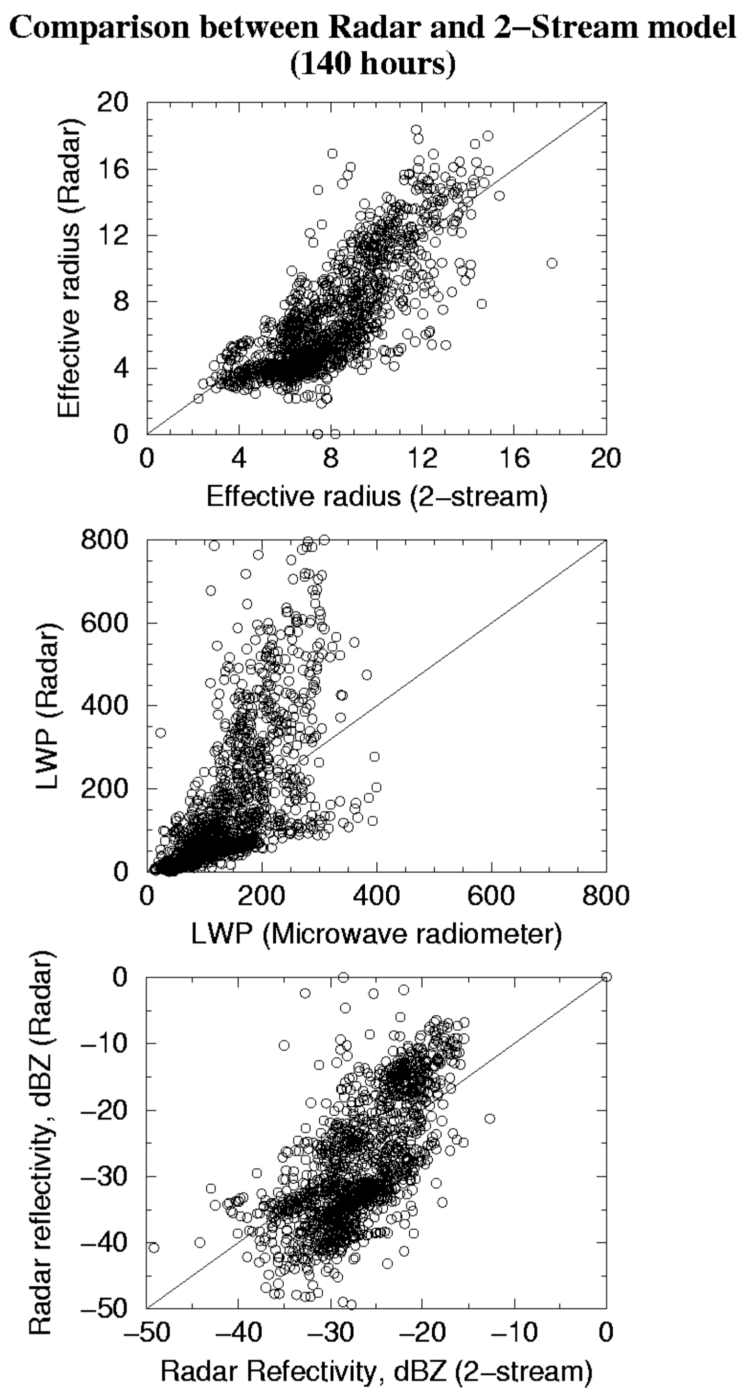

Figure 10. Summary of results from both M1 and M3 based on 140-hour data set.